Electrochemistry

Electrochemical Control of the Photocurrent Direction in Intercalated DNA/CdS Nanoparticle Systems**

*Ron Gill, Fernando Patolsky, Eugenii Katz, and Itamar Willner**

In memory of Chava Lifshitz

The use of molecular[1–4] and biomolecular[5–7] assemblies that perform logic gate functions has attracted substantial interest directed toward information storage and processing. In these efforts, nanoparticles have been employed to switch the conductivity properties across interfaces.[8,9] The integration of biomaterials with nanoparticles as active hybrid components in bioelectronic systems is interesting, as the unique recognition properties of biomolecules are combined with the optoelectronic functions of nanoparticles.[10,11] Double-stranded DNA (dsDNA) could act as a matrix to assemble signal-triggered functional nanoparticle structures by binding molecular units to the dsDNA. The conductivity of DNA has been a subject of extensive controversy,[12] and it is accepted that DNA exhibits poor conductivity.[13] However, the conductivity of DNA could be controlled by appropriate ordering of the base sequence[14] or by the incorporation of redox-active intercalators into dsDNA.[15] Herein, we report the design of CdS nanoparticle/DNA conjugates on gold surfaces and describe the effects of intercalators and the applied potential on the photoelectrochemical features of the system. We demonstrate that the resulting photocurrent can be reversibly switched between cathodic and anodic directions by controlling the redox state of the intercalated species.

In a previous study,[16] CdS nanoparticles were linked to gold surfaces and low-value anodic photocurrents in the presence of a sacrificial electron donor were recorded. This photocurrent was explained to originate from CdS nanoparticles that were in intimate contact with the electrode, owing to a low surface coverage of the nanoparticles, and thus the DNA matrix acted only as a linker in this system. In the present study, a dithiol-tethered single-stranded DNA (ssDNA) molecule **1** was self-assembled on the surface of a gold electrode and then hybridized with a complementary dithiolated ssDNA **2** to yield a double-stranded DNA (Figure 1). The resulting surface was treated with CdS nanoparticles to yield a semiconductor nanoparticle interface linked to the surface of the electrode by the dsDNA (Figure 1a). The surface coverage of the different components on the electrode support was determined by quartz-crystal-microbalance (QCM) measurements on Au/quartz crystals and by complementary electrochemical experiments. The surface coverages of the ssDNA **1** and the dsDNA complex were determined by chronocoulometry using $[Ru(NH_3)_6]^{3+}$ as a redox label.[17] The surface coverage of **1** and the dsDNA were found to be 1.8×10^{12} molecules cm^{-2} and 1.46×10^{12} molecules cm^{-2}, respectively. From the frequency changes of the Au/quartz crystal upon the assembly of the CdS nanoparticles, their surface coverage was estimated to be 4.9×10^{11} particles cm^{-2}. Thus, approximately three units of dsDNA link a single CdS nanoparticle to the electrode surface.

Figure 2a, curve 1, shows the photocurrent action spectrum of the CdS nanoparticle/dsDNA system in the presence of triethanolamine, TEOA, as a sacrificial electron donor. A very low anodic photocurrent is observed. The intercalation of doxorubicin (**3**) into dsDNA is well-established.[18] The intercalation of **3** into the dsDNA here results in a fivefold higher photocurrent (Figure 2a, curve 2). The electrolyte solution in the photoelectrochemical experiment is free of **3**, and the enhancement in the resulting photocurrent originates only from intercalated **3**. The coverage of the dsDNA with the intercalator **3** could not be assessed quantitatively, but differential pulse voltammetry experiments clearly indicated

[*] R. Gill, Dr. F. Patolsky, Dr. E. Katz, Prof. I. Willner
Institute of Chemistry
The Hebrew University of Jerusalem
Jerusalem 91904 (Israel)
Fax: (+972) 2-652-7715
E-mail: willnea@vms.huji.ac.il

[**] This research was supported by the EC STREP Project MOLDYN-LOGIC. This work is dedicated to Professor Chava Lifshitz, who passed away on March 1, 2005.

  DOI: 10.1002/ange.200500830

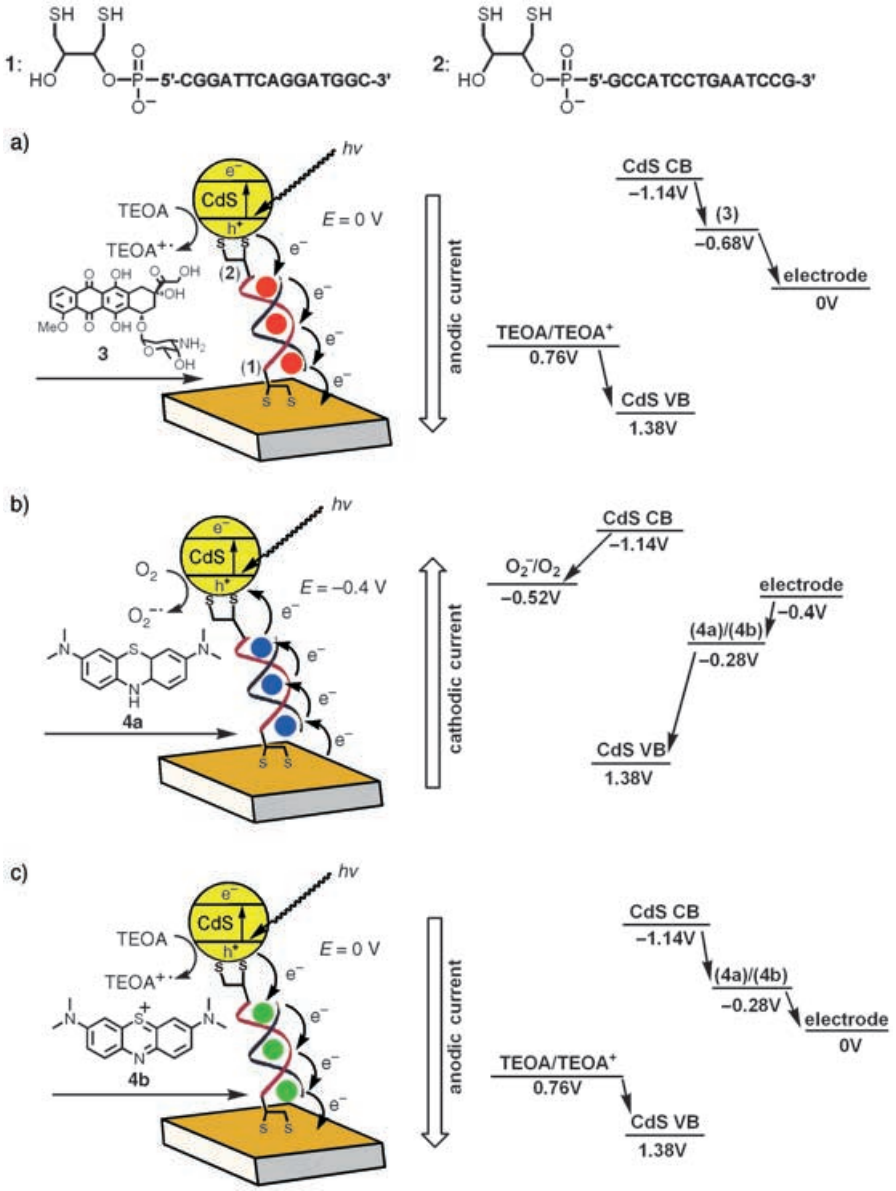

Figure 1. Directional electroswitchable photocurrents in the CdS nanoparticle/dsDNA/intercalator system. a) Enhanced generation of an anodic photocurrent in the presence of the doxorubicin intercalator (**3**; applied potential $E = 0$ V). b) Enhanced generation of a cathodic photocurrent in the presence of the reduced methylene blue intercalator (**4a**; applied potential $E = -0.4$ V). c) Enhanced generation of an anodic photocurrent in the presence of the oxidized methylene blue intercalator (**4b**; applied potential $E = 0$ V). The redox levels of the components that participate in the different photocurrent-generating systems are presented on the right side of the scheme. TEOA = triethanolamine; CB = conduction band; VB = valence band.

the binding of **3** to the dsDNA ($E° = -0.68$ V at pH 7.0). The photocurrent action spectra (Figure 2a) follow the absorbance features of the CdS nanoparticles (Figure 2b) which implies that the photocurrents originate from the photoexcitation of the semiconductor nanoparticles. Control experiments indicate that in the absence of TEOA, or without the association of the CdS nanoparticles, no photocurrents are generated in the systems. The fact that no photocurrent is generated in the presence of doxorubicin ($\lambda_{max} = 480$ nm) when the CdS nanoparticles are excluded from the dsDNA assembly prohibits the possibility that the **3**/TEOA pair contributes to the observed photocurrents. Thus, the enhanced photocurrent in the system that consists of the dsDNA with intercalated **3** is attributed to charge transport of conduction-band electrons to the bulk electrode by the intercalated quinone **3** (Figure 1a). Photoexcitation of the semiconductor nanoparticles yields an electron–hole pair. The transfer of the conduction-band electrons to intercalated **3** facilitates charge separation and the transport of electrons to the electrode to yield enhanced photocurrents. The redox levels of the components that participate in the generation of the photocurrent are presented in Figure 1.[19]

In a second configuration of the CdS nanoparticle/dsDNA system we employed methylene blue (**4**) as intercalator[15,18] (Figure 1b and c). A cyclic voltammogram of the system demonstrated a reversible redox process of intercalated **4** ($E° = -0.28$ V at pH 7.0) that can exist in the reduced state (**4a**; $\lambda_{max} = 400$ nm) or oxidized state (**4b**; $\lambda_{max} < 665$ nm), depending on the applied potential. Coulometric analysis of the reduction wave indicates that the surface coverage of **4** is 3.8×10^{12} molecules cm^{-2}. This value translates to the association of about two to three units of **4** with each dsDNA linked to the electrode. Figure 2c depicts the resulting photocurrents in the CdS nanoparticle/dsDNA system under an applied potential of $E = -0.4$ V and in the presence of O_2 as a sacrificial electron acceptor, in the absence of the intercalator (curve 1) and in the presence of the intercalator (curve 2). At this potential, the intercalator **4** exists in its reduced leuko form, **4a**. Whereas in the absence of **4a** a very low photocurrent is detected, in the presence of the reduced intercalator **4a**, the photocurrent is approximately fourfold higher. Control experiments reveal that upon the elimination of oxygen or the CdS nanoparticles from the assembly, no photocurrent is generated in the system. The photocurrent observed in the system is in the opposite direction to that observed in the presence of **3**. Thus, the enhanced cathodic photocurrent observed in the presence of **4a** originates from facilitated electron transport by the reduced intercalator **4a** (Figure 1b). Photoexcitation of the

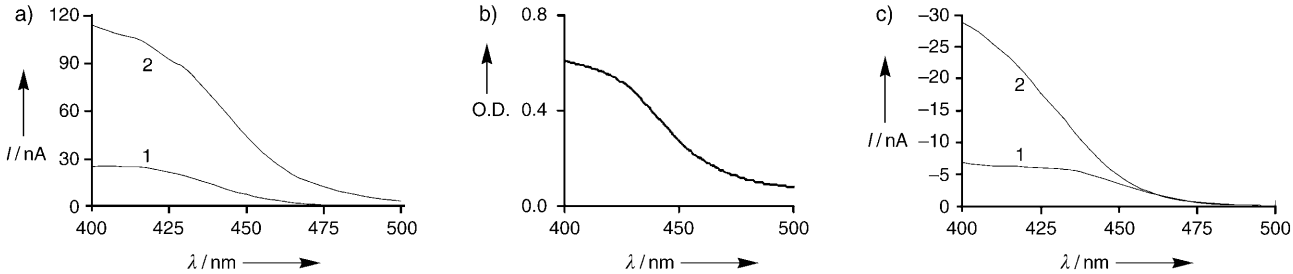

Figure 2. Photocurrent action spectra generated in the CdS nanoparticle/dsDNA systems: a) Anodic photocurrents generated in the absence (1) and in the presence (2) of the doxorubicin intercalator (**3**). The data were obtained at the applied potential $E = 0$ V and in the presence of TEOA (20 mM). b) Absorption spectrum of the CdS nanoparticles (OD = optical density). c) Cathodic photocurrents generated in the absence (1) and in the presence (2) of reduced methylene blue intercalator (**4a**). The data were obtained at the applied potential $E = -0.4$ V and in the presence of O_2 (under equilibrium with air).

semiconductor nanoparticles generates the electron–hole pair. Filling the valence-band holes with electrons that originate from the reduced intercalator **4a** facilitates charge separation and enables the enhanced reduction of O_2 by conduction-band electrons and the continuous generation of the photocurrent in the cathodic direction. The intercalation of the reduced methylene blue (**4a**) in the dsDNA allows charge transport from the electrode to the semiconductor nanoparticles, a process that leads to the effective generation of the cathodic photocurrent. Thus, the nature of the intercalator and its redox state control the direction of the photocurrent in the CdS nanoparticle/dsDNA/intercalator systems. The redox levels of the components that participate in the generation of the cathodic or anodic photocurrents are given in Figure 1.[19]

Inspection of the quasi-reversible cyclic voltammogram of the intercalated methylene blue (**4**) suggests, however, that one might use the same dsDNA intercalator for controlling the direction of the photocurrent by the application of an appropriate potential. That is, at an applied potential of 0 V, the intercalated **4** exists in its oxidized state **4b**, which behaves as electron acceptor. Thus, in the presence of the TEOA electron donor, an anodic photocurrent will be generated in the system (Figure 1c). Switching the potential on the electrode to −0.4 V yields the reduced state of the intercalator, **4a**, and in the presence of O_2 as electron acceptor the photocurrent will be switched to the cathodic direction (Figure 1b). Thus, in the presence of TEOA and O_2, one anticipates the possibility to switch the direction of the photocurrent by the applied potential. Switchable vectorial photocurrent generation was recently demonstrated by Yasutomi et al.[20] who employed helical peptides tethered to two different chromophores that acted as acceptor or donor units, respectively, upon photoexcitation. In contrast to their system, which requires the use of different wavelengths to switch the direction of the photocurrent, our system uses a dsDNA template and an intercalator to switch the direction of the photocurrent by alteration of the applied potential. Figure 3 shows the potential-induced switching of the direction of the photocurrent using the CdS nanoparticle/dsDNA system and either **4a** or **4b** as the intercalator. Photoexcitation of the system at $\lambda = 405$ nm results in an anodic current that is switched "on" and "off" by light at an applied potential

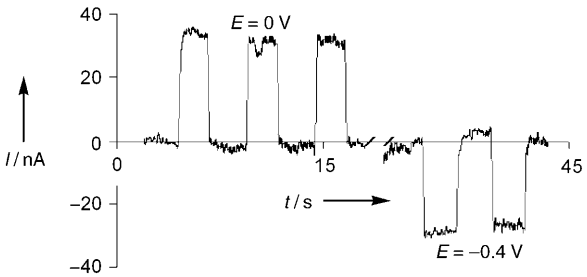

Figure 3. Electrochemically switched anodic and cathodic photocurrents generated in the CdS nanoparticle/dsDNA/**4b** (or **4a**) systems at 0 V and −0.4 V, respectively, in the presence of TEOA (20 mM) and O_2 (under equilibrium with air). Photocurrents were generated upon irradiation at $\lambda = 405$ nm.

of 0 V. Turning the applied potential to −0.4 V switches the photocurrent to the cathodic direction. The electroswitchable directional generation of the photocurrent is reversible and controlled by the applied potential.

The photocurrent generated by the CdS nanoparticle/dsDNA with the use of the intercalators corresponds to an AND logic gate, in which the photocurrent is generated only if the optical signal and the intercalator are introduced as activation stimuli to the system. The potential-controlled generation of the photocurrent in the **4a**/**4b**-intercalated CdS nanoparticle/dsDNA system not only allows the direction of the output current to be controlled but also allows regulation of the extent of opening of the gate and the resulting magnitude of the photocurrent.

To conclude, the present study has demonstrated the use of CdS nanoparticle/dsDNA assemblies on an electrode for the potential-induced switching of the directions of the photocurrents. The dsDNA acts as the template for the accommodation of the intercalators and its electrical contacting with the electrode.

Experimental Section

Dithiolated ssDNA (**1** and **2**) were prepared in situ during oligonucleotide synthesis using dithiophosphoamidite (Glen Research Inc.) by Sigma-Genosys Inc. DNA strands **1** and **2** were then reduced with dithiothreitol (DTT) and purified on a Sephadex G-25 column prior

to the modification of the surfaces. CdS nanoparticles (5.5 nm) were prepared in water using polyphosphate as a capping agent.[21] Glass slides (AF-45) coated with a 250-nm thick layer of gold (Evaporated Coatings Inc) were used as working electrodes. The Au electrode was modified using reduced **1** (10 μM) for 2 h in phosphate buffer (50 mM, pH 7.4) containing NaCl (0.5 M). The electrode was then washed three times with phosphate buffer (0.1M, pH 7.4) and modified with mercaptohexanol (1 mM) in water for 10 min to prevent nonspecific absorption of DNA on the surface. For the hybridization step, the **1**-functionalized electrode was treated with reduced **2** (10 μM) for 2 h in phosphate buffer (50 mM, pH 7.4) containing NaCl (0.5 M). The dsDNA- (**1**·**2**)-functionalized gold electrode was washed three times with phosphate buffer (0.1M, pH 7.4) and incubated in a solution of CdS (50 nM) for 12 h. Doxorubicin (**3**) or methylene blue (**4**) intercalators were incorporated into the dsDNA/CdS nanoparticle assembly by the interaction of the modified electrodes with a 50 μM solution of **3** or **4**, respectively, for 30 min, followed by rinsing of the electrode with phosphate buffer (0.1M, pH 7.4). Electrochemical and photoelectrochemical measurements were performed as described previously.[22] The photocurrents were measured in phosphate buffer (0.1M, pH 7.0) in the presence of either TEOA (20 mM) or oxygen (under equilibrium with air) or both. The working electrode area was 2.1 cm^2. All reported photocurrents represent the difference between the currents observed under light and dark conditions. The electrical potentials are reported relative to the saturated calomel electrode (SCE).

Received: March 6, 2005
Revised: April 13, 2005
Published online: June 23, 2005

Keywords: DNA · electrochemistry · intercalations · nanostructures · semiconductors

[1] A. P. de Silva, *Nat. Mater.* **2005**, *4*, 15 – 16.
[2] A. P. de Silva, N. D. McClenaghan, *Chem. Eur. J.* **2004**, *10*, 574 – 586.
[3] V. Balzani, A. Credi, M. Venturi, *ChemPhysChem* **2003**, *4*, 49 – 59.
[4] F. M. Raymo, *Adv. Mater.* **2002**, *14*, 401 – 414.
[5] M. N. Stojanovic, D. Stefanovic, *Nat. Biotechnol.* **2003**, *21*, 1069 – 1074.
[6] I. Willner, S. Rubin, *Angew. Chem.* **1996**, *108*, 419 – 437; *Angew. Chem. Int. Ed. Engl.* **1996**, *35*, 367 – 385.
[7] I. Willner, *Acc. Chem. Res.* **1997**, *30*, 347 – 356.
[8] D. I. Gittins, D. Bethell, D. J. Schiffrin, R. J. Nichols, *Nature* **2000**, *408*, 67 – 69.
[9] G. K. Ramachandran, T. J. Hopson, A. M. Rawlett, L. A. Nagahara, A. Primak, S. M. Lindsay, *Science* **2003**, *300*, 1413 – 1416.
[10] E. Katz, I. Willner, *Angew. Chem.* **2004**, *116*, 6166 – 6235; *Angew. Chem. Int. Ed.* **2004**, *43*, 6042 – 6108.
[11] C. M. Niemeyer, *Angew. Chem.* **2001**, *113*, 4254 – 4287; *Angew. Chem. Int. Ed.* **2001**, *40*, 4128 – 4158.
[12] D. Porath, G. Cuniberti, R. Di Felice, *Top. Curr. Chem.* **2004**, *237*, 183 – 227.
[13] P. J. De Pablo, F. Moreno-Herrero, J. Colchero, *Phys. Rev. Lett.* **2000**, *85*, 4992 – 4995.
[14] M. A. O'Neill, J. K. Barton, *J. Am. Chem. Soc.* **2004**, *126*, 11 471 – 11 483.
[15] T. G. Drummond, M. G. Hill, J. K. Barton, *Nat. Biotechnol.* **2003**, *21*, 1192 – 1199.
[16] I. Willner, F. Patolsky, J. Wasserman, *Angew. Chem.* **2001**, *113*, 1913 – 1916; *Angew. Chem. Int. Ed.* **2001**, *40*, 1861 – 1864.
[17] A. B. Steel, T. M. Herne, M. K. Tarlov, *Anal. Chem.* **1998**, *70*, 4670 – 4677.
[18] *Small-Molecule DNA and RNA Binders* (Eds.: M. M. Demeunynck, C. Bailly), Wiley-VCH, Weinheim, **2003**.
[19] a) M. I. Bodnarchuk, M. V. Kovalenko, A. L. Stroyuk, S. Y. Kuchmii, *Theor. Exp. Chem.* **2004**, *40*, 287 – 292; b) T. Akiyama, S. Nitahara, S. Inoue, S. Yamada, *Photochem. Photobiol. Sci.* **2004**, *3*, 26 – 28.
[20] S. Yasutomi, T. Morita, Y. Imanishi, S. Kimura, *Science* **2004**, *304*, 1944 – 1947.
[21] Y. Tian, C. Wu, J. H. Fendler, *J. Phys. Chem.* **1994**, *98*, 4913 – 4918.
[22] E. Granot, F. Patolsky, I. Willner, *J. Phys. Chem. B* **2004**, *108*, 5875 – 5881.

